

OPERATING EXPERIENCE WITH THE CRYOGENIC SYSTEMS FOR A SUPERCONDUCTING CYCLOTRON\*

M.L. Mallory, H. Laumer, D. Poe, P. Brindza  
 Cyclotron Laboratory, Michigan State University  
 East Lansing, MI 48824

Summary

The successful operation of the superconducting cyclotron cryogenic system has been primarily dependent on understanding and improving its performance. In particular, operating experience with a superconducting magnet coil, a vacuum cryopanel, and a cryogenic distribution system has been gained during the past three years. The coil cryostat cooldown, boiloff rate, warm-up, eddy current pulse, median plane heat leak, and helium leakage into the cryostat vacuum jacket have been measured. The vacuum cryopanel cooldown rate, heat load, pumping speed and long term gas storage have been determined. The present measurements have been conducted with simple independent transfer lines. A sub-cooled cryogenic distribution system, with parallel branches, has been designed and is presently under construction.

Introduction

The general characteristics and initial operating experience of the cryogenic system for the Michigan State University superconducting magnet has been described in a previous paper.<sup>2</sup> This paper describes the most recent operating experience with the magnet cryostat and the results of a prototype cryopanel for the cyclotron vacuum system. In the completed cyclotron, a liquid helium distribution system must be built to deliver liquid helium to the various systems and its design is presented in the last section. The large use of cryogenics is a major part of this recent technological development in cyclotrons.

Magnet Cryostat

Over three years operating experience of the magnet cryostat has now been acquired. Various performance parameters have been measured before the cryostat was disassembled to build the extraction system penetration channels through the median plane of the liquid helium cooled coils, as well as after the cryostat reassembly. The cryostat is now in its final configuration and no more changes which affect its cryogenic performance are expected. Figure 1 is a schematic drawing of the cryostat and the instrumentation used in measuring its performance; namely, platinum thermometers, liquid helium level gauges, vacuum jacket ionization gauge and a helium mass spectrometer.

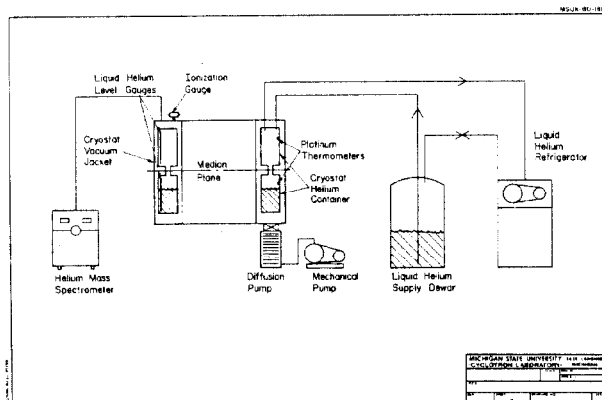


FIG. 1. A schematic drawing of the superconducting cyclotron showing the various monitoring devices used in making cryogenic measurements.

Cooldown-Warmup

Figure 2 shows the cooldown and warmup curves of temperature vs. time for the cryostat. The cooldown takes 120 hrs, and its rate is determined by the mass flow limitation of the refrigerator coldbox. The warmup of the cryostat is done by using the refrigerator to flow warm gas (~100K warmer than the coil) through the coil and returning it directly to the compressor pump suction, thereby bypassing the mass flow limitation of the refrigerator. The coil is warmed to room temperature in ~50 hrs.

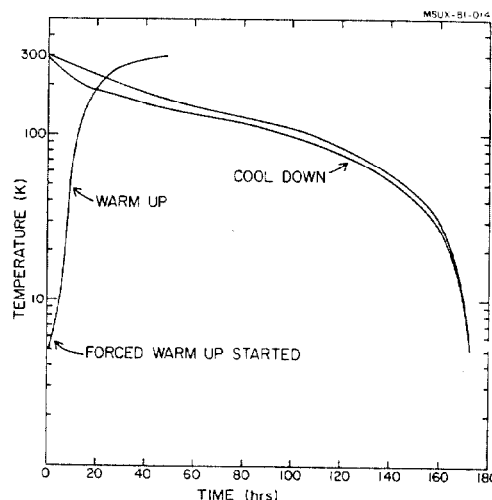


FIG. 2. The cooldown and warmup curves of the ~8 ton cryostat is shown. The cooldown is limited by the mass flow of the refrigerator.

Heat-Load

The heat load sources of the cryosystem are the transfer lines, storage system and the cryostat. The total load is less than 72 watts and more than 57 watts, determined by running the CTI 1400 refrigerator with two helium compressors and with and without liquid nitrogen.<sup>3</sup> The cryostat contribution to the heat load has been measured by monitoring its boiloff rate (Figure 3). It is 22 watts when the cryostat is filled to its operating level. An additional heat load due to the current leads when the magnet is at full current, is estimated to be 2 watts. In addition there is a transient heat load due to eddy current heating in the coil banding. Figure 4 shows how charging the magnet raises the helium level in the cryostat. It is proposed that the heating makes helium bubbles which then raise the helium level. A calculation of the expected thermal energy due to eddy currents is consistent with the amount of helium boiled, as estimated from the level increase. Details of the magnetic field change are consistent with the different rates of heating seen in charging and discharging the magnet.

Helium Leak

A helium leak from the coil cryostat to its vacuum jacket was detected. Figure 5 is a measurement of the pressure in the cryostat vacuum jacket; with a diffusion pump on, a pressure of  $4.6 \times 10^{-5}$  Torr had been attained; then the pump was closed off. A pressure increase with time indicating a helium leak rate of  $10^{-10}$  g/s was observed. Experimental data were acquired

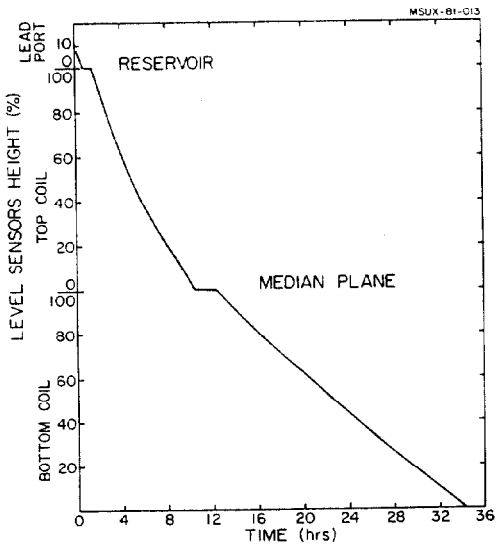


FIG. 3. The liquid helium boiloff curve of the magnet cryostat is shown. Three level sensors are used to measure the liquid helium level in the coil cryostat, with missing sensors at the reservoir and the median plane. Calculations based on boiloff rate correlated with liquid helium level allows the determination of the heat load from various sources. The total cryostat heat load, measured when it is filled to its operating level is <23 watts.

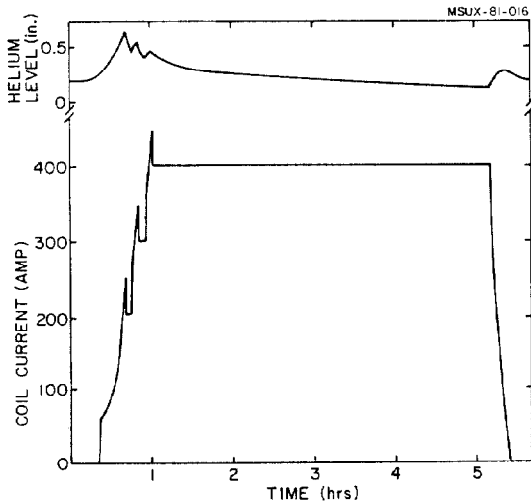


FIG. 4. The sudden increase in the helium level in the magnet (top curve) is correlated with the coil current as the magnet is charged and discharged. This increase is attributed to eddy current heating in the coil banding. The current spikes are related to the current, sent through only the dump resistor.

over 3 years and it was discovered that leaks in the upper part of the cryostat could be pinpointed by flowing cold gas through the different exit ports. However, for leaks in the lower part of the cryostat, it was discovered that the vertical location could be determined by monitoring the helium content in the vacuum jacket as the liquid helium level was changed. Figure 6 shows the signal detected for a leak in the cryostat median plane. Finally the bottom curve in Figure 5 is the response after fixing this leak, and now no diffusion pump need be used on the magnet cryostat vacuum jacket.

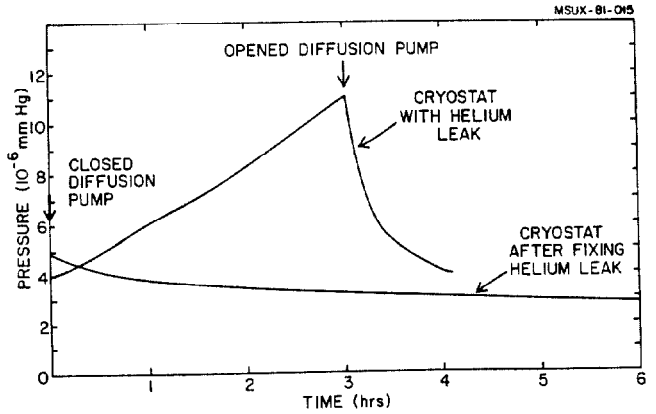


FIG. 5. The cryostat vacuum jacket pressure as monitored before and after fixing a helium leak. The cryostat now operates with no diffusion pump on its vacuum jacket.

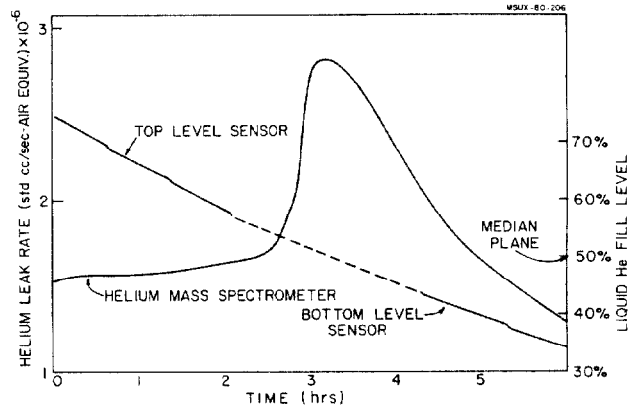


FIG. 6. The helium concentration in the vacuum jacket and the decreasing liquid level as a function of time are shown. Above the median plane, the helium concentration increases by about 2 and then decreases. This change in helium concentration is attributed to uncovering a leak channel in the cryostat by the liquid helium.

### Cryopump

A prototype cryopanel for the cyclotron was built and tested. Figure 7 is a drawing of the cryopanel and a cross section of the transfer line. The cryopanel will be mounted inside the dee and this necessitates the

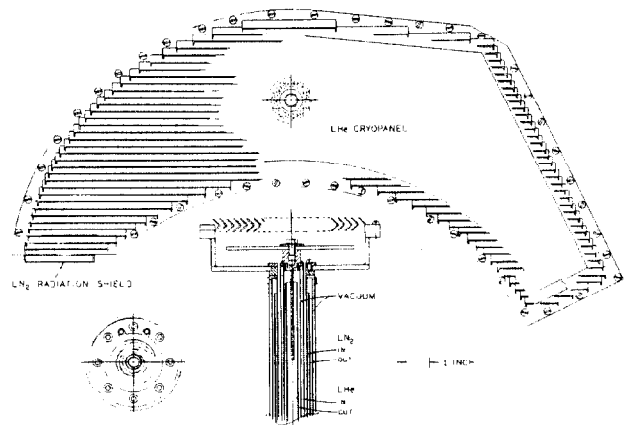


FIG. 7. A cross sectional view of a cyclotron cryopanel and a section of the transfer line. The pumping speed for nitrogen is 4000 l/sec.

construction of a coaxial transfer line (17 ft) through the rf center conductor stem. A vacuum space is inserted between the feed and return line of both the liquid helium and liquid nitrogen system in the transfer lines, thereby avoiding heat exchange between feed and return and thus allowing rapid cooldown of the panel.

Figure 8 is the cooldown curve of the cryopanel, where the temperature at various points has been measured and indicates that the liquid helium cooled surface takes 2 hrs to reach 20K. The heat load of the cryopanel and its transfer lines was less than 23 watts.<sup>3</sup> The pumping speed of the cryopanel in a test chamber has been measured for both nitrogen and neon gas and is 4000 l/sec. In addition a long pumping test was performed where nitrogen gas at the expected ion source feed rate of (1 cc/min) was flowed into the test chamber and the facility operated for 20 days with no degradation in pumping speed.

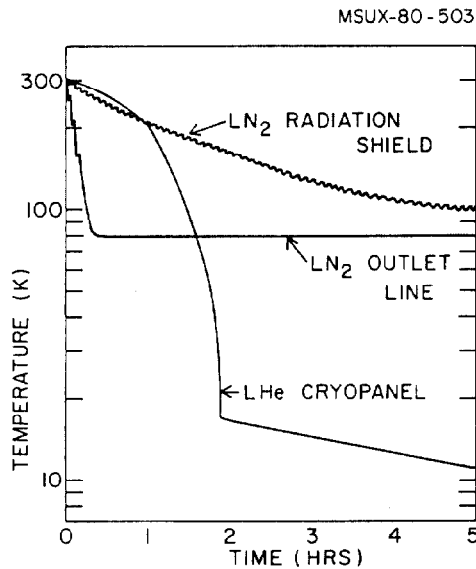


FIG. 8. The cooldown measurements of the cryopanel. In 2 hrs the cryopanel temperature was below 20K. The rate of cooldown below 15K is limited by the black body radiation from the liquid nitrogen shield.

### Cryolines

A schematic layout of the cryolines for the cyclotron is shown in Figure 9. The system will have a main branch with each load feeding from this subcooled line. It is expected thus that single phase liquid helium will

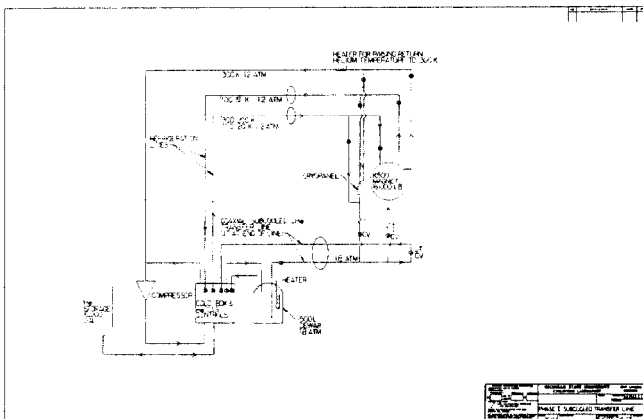


FIG. 9. A schematic piping diagram of the liquid helium distribution system. The main liquid helium line will be subcooled.

then flow to each device, thereby alleviating two phase control problems and turbulence. In addition, the helium lines will be shielded with LN<sub>2</sub>, to reduce the thermal load. The sizes of the lines are determined by transient conditions, i.e. cooldown; typical piping sizes for our system are shown in Table 1. In the steady state operation, signals from silicon diode temperature sensors and from differential pressure sensing devices will be interpreted by decision making modules, which will control pneumatic transducers that operate fluid control valves.

Table 1. Cryoline parameters.

FLUID TYPE	MASS FLOW ( $\frac{g}{s}$ )	FLUID PRESSURE (atm)	FLUID TEMP (K)	PIPE DIAMETER (in)
He(1)	15	1.2	300	2.0
He(2)	3	1.2	100	0.75
He(3)	2.9	1.8	4.9	0.25
He(4)	2.9	1.2	4.4	0.5
N <sub>2</sub> (5)	23.6	1	300	2.0
N <sub>2</sub> (6)	51	1	77	0.65

The calculations are appropriate for:

- (1) warm He gas returned to compressor or He gas used to cool down the magnet from 300 K;
- (2) cold He gas returned to refrigerator;
- (3) the sub-cooled liquid He line;
- (4) the He bath for the subcooled line
- (5) the N<sub>2</sub> boil off gas during magnet cooldown;
- (6) the liquid N<sub>2</sub> supply line assuming a maximum flow rate of 1 gal/min.

### References

1. H.G. Blosser, IEEE Trans. Nucl. Sci., NS-26, No. 2, 2040 (1978).
2. M.L. Mallory, IEEE Trans. Nucl. Sci., NS-26, No. 2, 2138 (1978).
3. C.T.I. Operator's Manual for Helium Refrigerator/Liquifier Model 1400 for M.S.U. 4-15 (1976).
4. M.L. Mallory and H.G. Blosser, Nucl. Instr. and Meth., 155, 573 (1978).
5. M.L. Mallory and H.W. Laumer, Nucl. Instr. and Meth., 177, 481 (1980).